



Journal of Advanced Research in Applied Sciences and Engineering Technology

Journal homepage:
https://semarakilmu.com.my/journals/index.php/applied_sciences_eng_tech/index
ISSN: 2462-1943



Inscribing the Compositional Changes of Heterogeneous Bio-system through FTIR Spectroscopy – Demonstration of Guideline to Sound Interpretation

Arniza Ghazali^{1,2,3,*}, Nur Haffizah Azhar¹

¹ Division of Bioresource Technology, School of Industrial Technology, Universiti Sains Malaysia, Penang, Malaysia

² Green Biopolymer, Coatings & Packaging Cluster, School of Industrial Technology, Universiti Sains Malaysia, Penang, Malaysia

³ Renewable Biomass Transformation Cluster, School of Industrial Technology, Universiti Sains Malaysia, Penang, Malaysia

ARTICLE INFO

Article history:

Received 15 November 2022

Received in revised form 7 December 2022

Accepted 29 December 2022

Available online 20 January 2023

Keywords:

FTIR; Spectroscopy; Nanoscale; Biomass; Crystallinity; Bio-silicates

ABSTRACT

Fourier transform infrared (FTIR) is a powerful technique of chemical structural elucidation for pure compounds but demanding for heterogeneous samples. Configuration with a complete spectral library supports auto-elucidation simply by matching with the spectral database. The technique is highly accurate for a pure, totally unknown organic sample but no more than an approximation for a complex macromolecule or a mixture of compounds due to the poor selectivity or the inability to differentiate C-H variations. Spectral complexity increased with sample heterogeneity due to the responses from inter-atomic or molecular bond vibrations, making analysis demotivating enough to prompt analyst to duplicate interpretation. This study demonstrates a stepwise guide for interpreting the FTIR output. Comparative analysis of signals laid on a spectral overlay was demonstrated, followed by band assignment based on assimilated literature and underlying reactions. Scrutiny on the critical spectral regions required sound FTIR interpretation of heterogeneous samples to arrive at an adequate scientific understanding of the underlying reactions. With a justified choice of band, samples' relative crystallinity determined via FTIR approximated those derived from the x-ray diffraction (XRD) spectroscopy. Beyond crystallinity, the calculated indices may also be the markers of certain reactions and sufficient replication could be used to define the route of the extent of the reactions. Adopting the recommended steps allowed a comprehensive understanding of scientific work. The findings signal FTIR's suitability for robust analysis of heterogeneous samples with the level of accuracy dependent on the depth of data harvest and sound theory-backed interpretation.

1. Introduction

Vibrational spectroscopy is a low-energy and low-cost technique of ultra-high accuracy and precision analyses. Its applications have gone beyond purity analysis in the manufacturing sector but gained a prominent call for rapid and non-invasive diagnostic tools for cancer [1], HIV [2],

* Corresponding author.

E-mail address: arniza@usm.my

<https://doi.org/10.37934/araset.29.2.276290>

diabetes and periodontitis [3]. With technical push and clinical friendliness [4], the inexpensive, rapid FTIR analysis will be the sought-after non-invasive medical diagnostic tool in no time. Besides structural elucidation of pure chemicals, the analytical reliability of the heterogeneous sample analyses is now possible with software-assisted structural elucidation, quantitative analysis, and image analysis making analysis handier than ever.

Equally heterogeneous is the fibrous biomass ensuing 85% of the global edible oil [5], attracting the global research on utilisation. In inscribing the invisible changes, FTIR came as an eye for structural studies on the domiciling supra-molecule. With Malaysia's record high MYR102 billion export worth of oil [6] are the countless constituent commodities, entitling the edible botanic oil sector to weave symbiosis with the cosmetics and health industries [7]. Post-harvest of the oil fruit bunch, the complementary 90% portion consists of residual fibrous mass [8] accounting for some 35 million tonnes of the oil palm empty fruit bunch also as a commodity for other production lines. Pre-processing of the bunch structure by depithing yields valuable vascular bundles called the empty fruit bunch (EFB) housing the supra-molecular components in Figure 1.

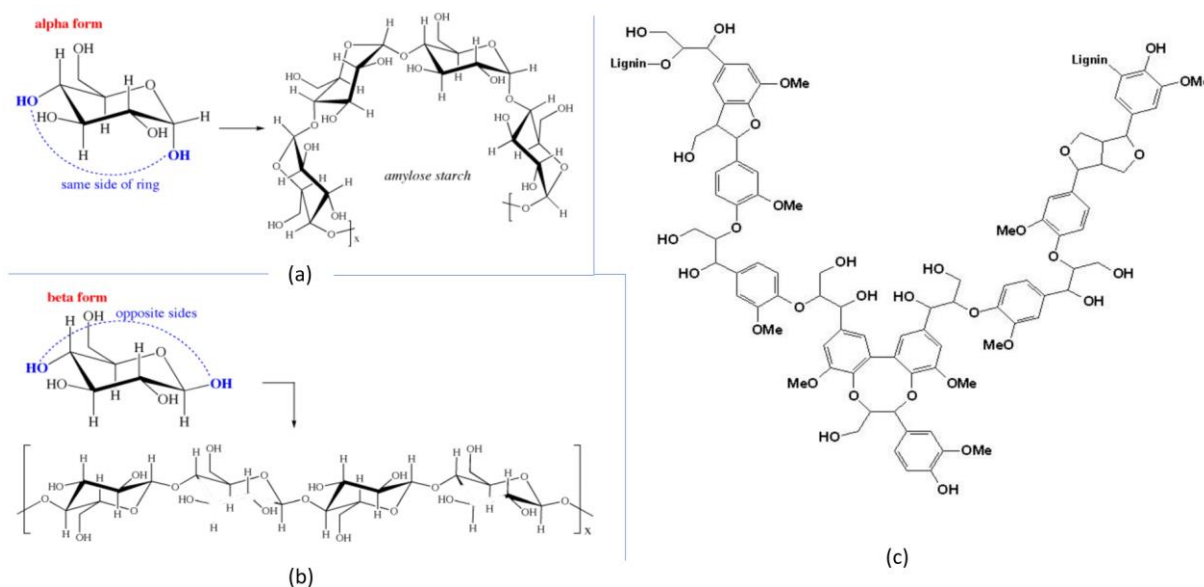


Fig. 1. The component of biomass is a heterogeneous mix of (a) hemicellulose (b) cellulose as the predominant component and (c) lignin, hailing biomass as lignocellulose and the less said others. Reproduced from <https://butane.chem.uiuc.edu>

Besides the principal components in Figure 1, non-dominant structures with similar functional groups are tannins and alkaloids. Zooming into individual cellulosic fibres reveals the presence of such quinones as the 2,5-dihydroxyacetophenone and similar isomers. In chemical pulp, which is reputed for purity, 2,5-dihydroxyacetophenone was detected at a trace, ppb level, suggesting the presence of residual lignin [9,10].

The biomass of focus in this study is the oil palm empty fruit bunch (EFB) and the extracted impure fibres. Unlike the fibres from the lignin-removing process, the less reviewed ones are the semi-chemical pulp generated by the relatively new, high-yield alkaline peroxide pulping. The technique is dubbed as the solution to the polluting chemical pulping principle and the 2-in-1 pulping-in-bleaching outcome helped reduce the capital otherwise required for a chemical system with a separate bleaching plant. Offering pulp properties comparable to a chemical pulp [11] with a unique mass of useful fines, making zero-waste and resource efficiency [12] an actualised pillar. The high-yield fibres are particularly unique with retained radical-altered lignin fragments (RADIALS) with such other

components as vanillin [13] and carotenoid [14] recognised as extractable. Despite the impurities, the fibres could be deconstructed to nano-scale cells that could functionalised food via desirable coating effects. Besides food, the generated cells also enabled precision printing engendered by nano-capillary effects of TRX-cells' fibrillary ends [15]. Its compatible use as a transport [16] agent for bio-pigment, are scores for its potential use as the bio-nanocarriers in controlled-release drug delivery analogous to nano-chitosan counterpart [17].

Owing to the unique TRX-cells and microfibre composition, the duo is selected in outlining the systematic guideline for interpretation of FTIR of heterogeneous samples – a good pick for interpretation due to its bizarre properties in comparison to the commonly discussed cellulose nano-fibres. Additional analysis of crystallinity is also discussed relative to XRD crystallography for insight into data discrepancy and to testify the trend in crystallinity values derived using FTIR. With the details combined, this study aims to outline the steps for FTIR spectral interpretation involving complex or heterogeneous samples via selective literary analysis beyond the identification of functional groups.

2. Methodology

2.1 Sample Preparation

The oil palm empty fruit bunches (EFB) vascular bundles were reacted at 70°C in a water bath with sodium hydroxide premixed with hydrogen peroxide. The generated dioxydanyl radical reacts with the chromophoric groups of plant biomass to form photostable organic molecules. The bright resultant biomass spawning from the fascinating reaction principle makes it widely used in pulp production and bleaching processes [18] troubleshooting the environmental impact of chlorine bleaching and sulfur-based fibre extraction process. The 2-in-1 bleaching-and-pulping process commensurate with the resource efficiency principles or circularity [12] at the least, the economy from being a time-saving process. For demonstrating an objective analysis of the sample, experimental conditions were kept well controlled to yield clean spectra [19] devoid of unintended noise so that all detected changes are the target observations.

2.2 Spectroscopy: FTIR and XRD Analyses

FTIR spectra of the cellulosic samples (EFB feedstock, dioxydanyl-reacted refined EFB ('m-fibres' or microfibrils) and PFI-milled mass) were acquired using the Perkin Elmer's Frontier FT-IR/NIR interfaced with MIR-TGS detector and UATR accessories. A total of 16 cumulative scans were taken, at a resolution of 8 cm⁻¹, in the default frequency range of 4000-650 cm⁻¹. The transmittance versus wavenumber spectra was converted to Absorbance (Abs) spectra based on the Abs values pre-converted by Sigma-Aldrich. Crystallinity values were then derived from the ratio between two sets of band intensities, Absorbances at 1370 cm⁻¹ to that at 2900 cm⁻¹ Eq. (1) and the ratio of Abs corresponding to 1430 cm⁻¹ to that occurring at 893 cm⁻¹ Eq. (2):

$$\text{Crystallinity (1)} = [\text{Abs}_{1372}/\text{Abs}_{2900}] \times 100 \quad (1)$$

$$\text{Crystallinity (2)} = [\text{Abs}_{1430}/\text{Abs}_{893}] \times 100 \quad (2)$$

Considering the heterogeneity of the reaction system involving biomass and the low selectivity of FTIR as an instrumental analysis, the ratio between the varying band intensities corresponding to

the signals corresponding to hydroxyl stretching at 3300 cm^{-1} and those in the vicinity of 1644 cm^{-1} were also compared.

To ascertain the theoretical effects of dioxydanyl radical on EFB, the biomass in the form used as the reaction precursor, the dioxydanyl-reacted mass and the extensively refined mass were studied. The samples were ground and pelletised in a KBr disk for analysis using Frontier FT-IR/NIR Spectrometer at the Science, Engineering Research Centre (SERC), of the university's Engineering Campus in the mainland of Penang.

Vibrational analysis of the sample yielded a Transmission vs Wavenumber spectrum between 650 cm^{-1} to 4000 cm^{-1} wavenumbers. All comparisons were made in the spectral overlay. Triplicate data sets were prepared for analysis, with only one display on signal disappearance applying baseline correction.

Crystallinity was derived based on the two regions representing the crystalline structure of plant cellulose. They were absorbance at 1430 cm^{-1} , 893 cm^{-1} , 1320 cm^{-1} and 2900 cm^{-1} as proposed by Ciolacu and co-researchers (2011) [20]. Considerations were also made on the modification of the botanical chromophores by the dioxydanyl radical (DIOR).

The X-ray Diffractogram of the raw material, microfibre and the TRX-cells[®] were analysed to check the peaks and the related crystal planes. XRD was performed on a four-circle goniometer (XDS-2000 Poly-crystalline Texture Stress (PTS) goniometer; Scintag, Scintag Inc., Cupertino, CA, USA) using $\text{CuK}\alpha$ radiation generated at 45 kV and 36 mA. The $\text{CuK}\alpha$ radiation consists of $\text{K}\alpha_1$ (0.15406 nm), $\text{K}\alpha_2$ (0.154 nm) and the subtracted $\text{K}\beta_2$ (0.139 nm) component. The 0.5-1 mm slits were fixed for a 320 mm goniometer working radius to handle signals from approximately 0.5-1 g dried samples mounted onto a quartz stub. Scans were obtained from 5° to $40^\circ 2\theta$ in 0.05° steps or the rate of 15 seconds per step. Samples' crystallinity indices (CI) were calculated from the height ratio between the intensity of the crystalline peak ($I_{002} - I_{AM}$) and total intensity (I_{002}). The d-spacing values of major signals are calculated using Bragg's Law (mathematical equation) Eq. (3), while the crystallinity index is derived from Eq. (4).

$$\pi\lambda = 2d \sin\theta \quad (3)$$

$$\text{Crystallinity Index, CI} = \frac{(I_{002} - I_{AM})}{(I_{002})} \quad (4)$$

In the common cellulose nano fibres (CNF) production systems involving elevated chemical use on EFB, the highest crystallinity was offered by the pure cellulose and the lowest was portrayed by the biomass precursor [21-23]. The crystallinity values derived in this study are thus analysed via X-ray Diffractogram as well as the varying ways of expediting signals of the FTIR technique.

Due to the unique outcome of dioxydanyl radical reaction towards the chromophoric group, this study attempted to track compositional change from FTIR, projected to be assessing the amount of compliance with the splitting and reformation of hydrogen bonds arising from high alkalinity reaction proposed by [24].

2.3 Literature Selection

Articles on the FTIR, XRD, crystallinity, cellulose and lignin related to EFB were the main references gathered to align the theories related to step three of FTIR interpretation. The revised version of established Organic Chemistry textbooks was cross-referenced to check the validity of the signal assignment and works of silicates [25-27] were evaluated to explain the possible interference occurring in the analysis in focus. with the background information already established for EFB and

TRX-cells. was identified as a useful reference amongst all the references not specific to the identification of residual lignin in biomass fibre matrix. Nandiyanto and co-authors (2020) addressed signals corresponding peroxide related silicate [25], which indicates a strong link to the work in focus. While [28] Zwichmayr’s account on de-aromatisation (2018) serves to understand the underlying chemistry and heterogeneity added by isomerism, analysis of lignin moiety extracted from EFB established by Sun *et al.*, [29] has been an evergreen reference for the simpler lignin fragments present in EFB of the (general) units explicitly shown by Katahira as syringic, ferulic and guaiacyl [30]. The lignin-peroxide-specific investigation by Sun and co-workers (1998) provides relevant insight into the cleavage of the aromatic ring by peroxide [31]. The discussion on cellulose by Thulluri and co-researchers (2021) provides useful insight into IR-active cellulose polymer [32]. Crystallinity determination was based on the description [20, 33] of Ciolacu and team (2011) and Park (2012) and cross-checked with XRD crystallographic technique. Only works describing baseline correction and other calibrations are taken to discussion due to the susceptibility of crystallinity index to the spectroscopic parameters. The fundamentals of FTIR [34] described by Solomons and colleagues (2022) were cross-referenced to check for accuracy.

In essence, there are many methods for determining crystallinity XRD, TGA, NMR, and FTIR – this study recommends the simple FTIR technique with XRD for verification. The preceding analysis was condensed to demonstrate the steps in FTIR analysis of heterogeneous systems. As much as FTIR has become a prospectus technique in critical fields like medical diagnosis, the rapidity, reliability and precision should be maximised by scholars seeking to understand complex molecular systems on routine analysis.

3. Results

3.1 Initiation Steps in STraP

To develop a systematic protocol for structural analysis using FTIR, a spectral overlay of the feedstock (A), pre-treated feedstock (B), and the refined version of B (C) was generated and interpreted. The raw material or the feedstock, the oil palm empty fruit bunch, EFB was selected as the reaction precursor and reacted with alkaline peroxide. Theoretically, adding alkali to hydrogen peroxide in a correct sequence at 70°C (“cold system”) gave rise to the short-lived dioxydanyl radical, OOH· (Reaction 1, Figure 2). To generate powerful functional cells (TRX-cells®), EFB was first modified via DIOR and refined in a standard Andritz Bauer fibrillation system. Subsequent refinement was done using a PFI mill, abiding by the standard procedure in TAPPI standard method [35]. The summary of steps involved in DIOR-treatment of EFB (reaction 2, Figure 2) yielding TRX-cells® is as follows:

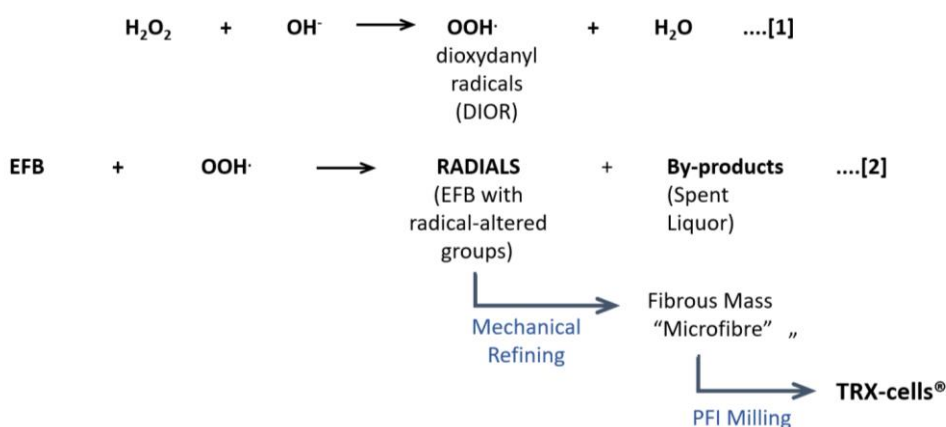


Fig. 2. The principal chemical and mechanical actions in TRX-cells® production.

FTIR spectra associated with the precursor, modified biomass and refined fibres were acquired. The first step in a compositional change analysis is to overlay the spectra and decide on the baseline correction. Figure 3 eliminates baseline correction to avoid crowding.

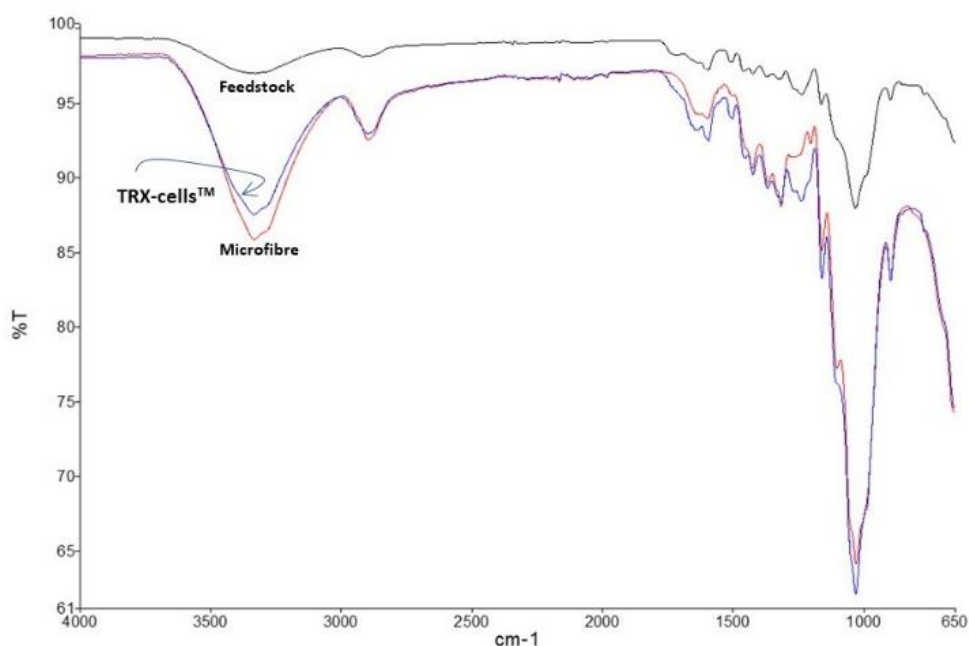


Fig. 3. Raw spectral overlay for EFB, microfibre and the TRX-cells® a refined product from reaction 2.

Fulfilling STraP, Figure 3 is then appropriately marked tracking for the features in Table 1. As the compositional changes in focus involved alteration of a portion of a macromolecule, signal shift, transmission intensity and changes in signal pattern (STraP) were expected.

In protein analysis aiming to detect the possible mutation, the signal shift is one of the important considerations. As a diagnostic tool, a two-wavenumber unit shift [1,2] could delineate cancerous from benign results and an HIV-positive from the rest, affecting medical decisions, subsequent interventions from the hospital and the cost borne by patients. Understanding the delineation points could avail an efficient diagnostic tool that not only speeds up diagnosis but could also save more lives than ever.

Table 1

Raw Meaning of Spectral Variations Suited for Complex Samples

Changing Feature	Plausible Occurrence
Signal shift (S)	<ul style="list-style-type: none"> - Effects of sample media/humidity on functional groups. - Interacting multicomponent sample.
Transmission Intensity (I)	<ul style="list-style-type: none"> - Signal cancelling. - Functional group transformation. - Intermolecular perturbation.
Band Pattern/Shape (P)	<ul style="list-style-type: none"> - Understanding the hugest response. - Signal disappearance. Change in chemical structure.

Trough disappearance is clearcut in synthetic products involving one or more reactants changing the chemical structure of a product. In a heterogeneous system not involving corrosive systems, changes are normally subtle. Taking the steps in Table 1 helps better visualisation of the proceeding needs.

Marking the features in Table 1 into Figure 2 and completing STraP (hereon denoted STRAP) yields Figure 4. Beyond signal assignment, the numbered signals transferred to Table 2 were evaluated in terms of intensity changes. The sample of delineation narratives are presented in section 3.3.

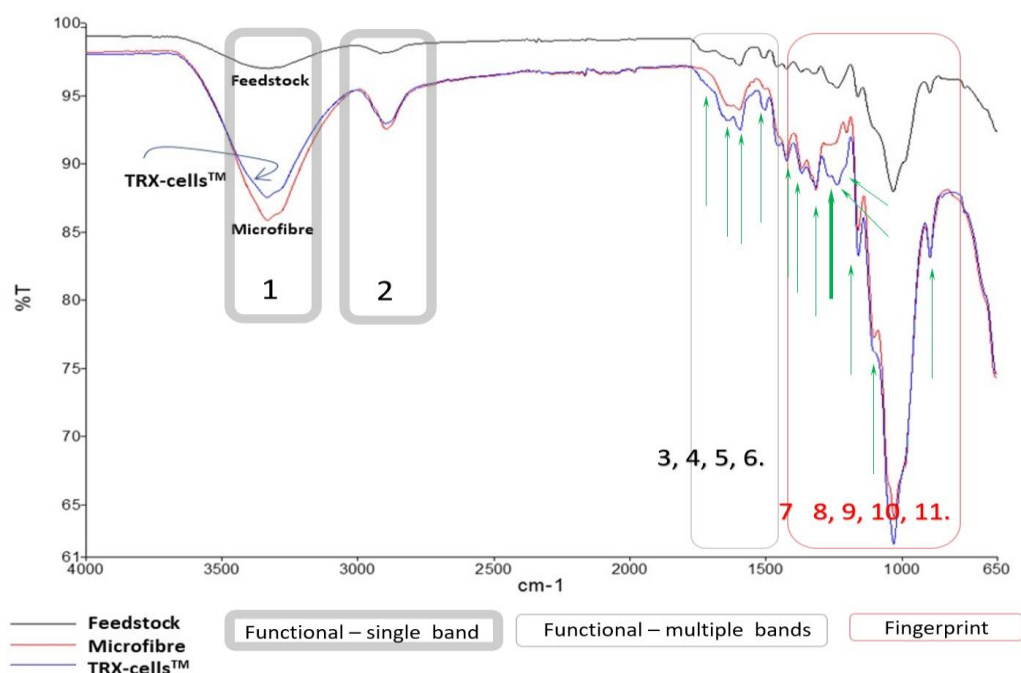


Fig. 4. Marked spectral overlay for illustration only

STRAP had identified 13 signal variations and the detailed analysis requires baseline corrections embedded in the discussion.

Table 2
 FTIR Active Bonds with delineation feature

	Bands (cm ⁻¹)	Signal Assignment	Delineation Feature
1.	3350	Cellulose (polymeric) OH stretch or OHIIIH	Pronounced μ -fibre > TRX cf. EFB
2.	2900	Linear C-H Methylene C-H ₂ [32]	μ -fibre & TRX >>> EFB -
3.	1750	C=O aromatic skeletal C-H	TRX (\approx EFB); absent for μ -fibre
4.	1650	C=O [25] aromatic skeletal[36]	TRX > μ -fibre > EFB
5.	1600	C=O conjugated ketone	TRX > μ -fibre > EFB (shadowed)
6.	1550	Carboxylate/carboxylic salt	TRX > μ -fibre > EFB (shadowed)
7.	1400-1450	Aromatic C-C vibration [29]	TRX > μ -fibre >> EFB
8.	1300-1200	Primary or secondary OH in-plane [25] Syringyl [36]	TRX (\approx EFB); absent for μ -fibre
9.	1275	Guaiacyl [36]	
10.	1150	Alkyl substituted C-O [25] Guaiacyl [36]	TRX > μ -fibre >> EFB
11.	1100	Alkyl substituted C-O or silicate [25]	TRX > μ -fibre >> EFB
12.	1037	Guaiacyl [36]	TRX > μ -fibre >> EFB
13.	1010	Alkyl substituted C-O or silicate (huge) [32] Guaiacyl [36]	TRX > μ -fibre >> EFB
14.	890-890	Silicate [25, 27, 32] Out-of-plane C-H bending [27] (meta-substituted aromatic ring)	Pronounced for μ -fibre and TRX

The column labelled “Delineation Features” was intended to offer the correct footing for analysis. The rest of the analysis demanded for active cross-checking of the literature, and if applicable, use of standards. As differences are spotted and evaluated to be significant, marking by highlighting (Items 10-13 in Table 2) helped identify the signals requiring further scrutiny. The hugest transmission band in Figure 2 are marked blue (Table 2) to alert the influential functional group in the sample.

Thus far, the checklist of tasks summarized as preliminary S-Tra-P (STRAP) followed by the first two delineation steps in Figure 4 are completed. Steps 3 and 4 determine the quality of reporting in step 5, the narratives of which are presented in the proceeding section.

3.3 Theoretical Accounts: Characterisation of TRX-cells®

This section serves as a guide for step three onwards in Figure 5. Given the unique nature of alkaline peroxide reactions that are susceptible to small experimental changes, a separate review had already been done to testify formation of dioxydanyl radical formation (Reaction 1) [11, 13, 16, 37]. Reactions 1, 2 and 3 are now the compass of the analysis.

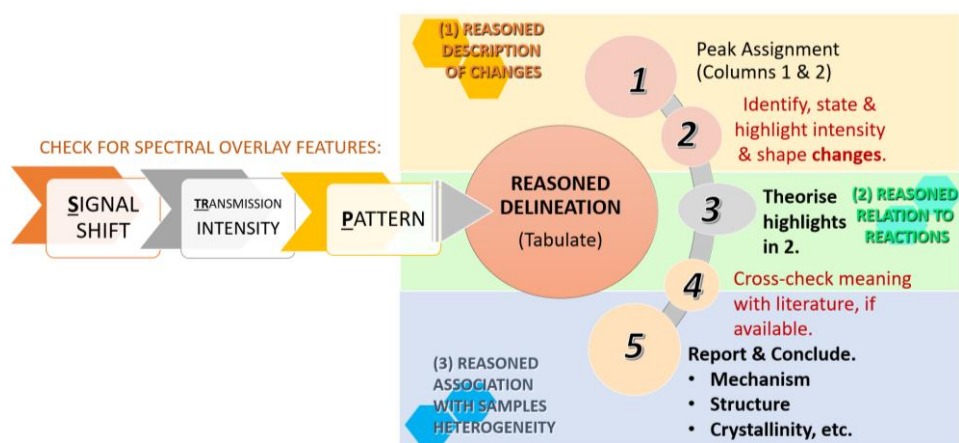


Fig. 5. Summary of the steps for careful initiation of FTIR spectral analysis of a heterogeneous system

3.3.1 Relations with previous works

The signal assignment of the materials in focus shows a major clue corresponding to the effects of dioxydanyl radical on EFB (Reaction 2). The effects were stable and somewhat unaffected by extensive mechanical milling. The trough at 820-890 cm^{-1} affirms the presence of peroxide-based silicate, which coincides with the elemental analysis performed with TEM [15]. The signal is also attributable to the out-of-plane bands associated with aromatics with the faint theoretical bands between 1605 cm^{-1} to 2000 cm^{-1} . The in-plane hydroxyl O-H band at 1300 cm^{-1} to 1200 cm^{-1} shows an enhancement in band size, commensurate with the RADIALS formation in reaction 2 but more predominantly these are attributed to the cellulosic O-H given the absence in the spectrum of microfibre.

With fragments of lignin macromolecules converting to RADIALS, the portion of the mass identified as photostable and active participants of inter-fibre bonding increased (Figure 6b), giving the possibility of an ordered structural arrangement and a high crystallinity.

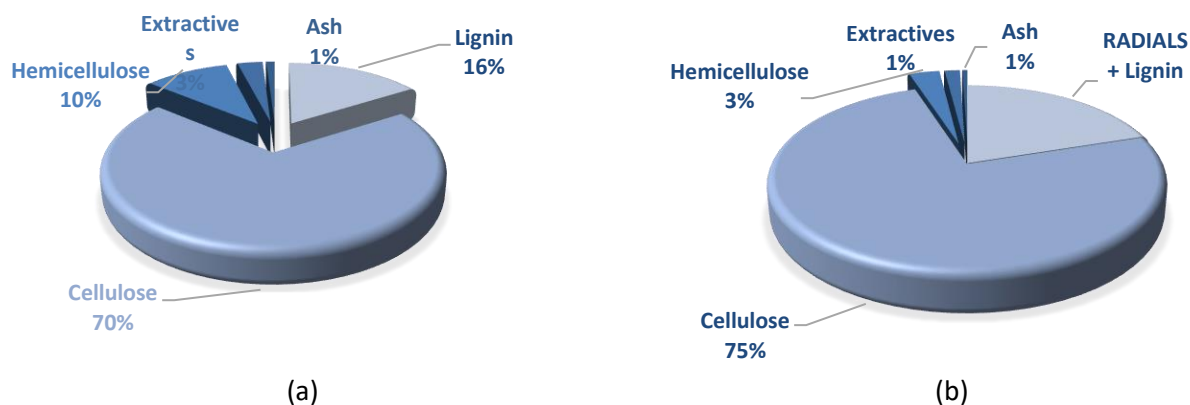


Fig. 6. Predominance of cellulose in EFB (a) at origin and (b) amidst the RADIALS

The huge peak in the hydroxyl region implies the hydrophilicity of TRX-cell® in line with analysis on its application as paper coat [15]. Exposure of the OH with extensive milling resulted in a hydrophilic surface having affinity to inkjet, hence improving inkjet printability significantly.

Dioxydanyl radical (DIOR) reaction with EFB appears to have attacked the chromophoric groups, producing RADIALS that are photostable and promoted inter-fibre bonding [11, 38, 39] at par with chemical fibre web. The well-defined signal at 3300 cm⁻¹ reflects the effect of phenolics, which were found to predominate [36] over aromatic cleavage shown in reaction 2 as also reported by Zwichmayr and team (2018) [28]. The contribution of the polyphenolic groups from residual tannic acid and the aforementioned carotenoids may also produce the feature.

The subtle C-H shoulder above 3000 cm⁻¹ which was indicative of hemicellulose (Hinterstoisser *et al.*, 2000) [40] suggests the negligible amount of hemicellulose, plausibly almost completely leached during the DIOR reaction and prior processing. Reaction associated with carbonyl with DIOR giving rise to the cleavage of the aromatic ring (reaction 3, Figure 7) may explain the significantly intense transmission band corresponding to C-H linear stretch at 2900 cm⁻¹ inclusive of methylene (Thulluri *et al.*, 2021) [32]. The initial chromophoric structure of EFB is predominantly syringic [29] and seems to correlate with the found scanty (<10%) yield in the mass of lignin moiety [34] (Figure 8a) of the reaction product forming via a mechanism in reaction 2. Similar encounter is portrayed in Figure 6b for the close-up analysis of the lignin related region in Figure 6a. At the current state, inference pivoted around the negligible RADIALS (reaction 3, Figure 7) forming, and thus, incompliance to the de-aromatisation of EFB lignin fragment.

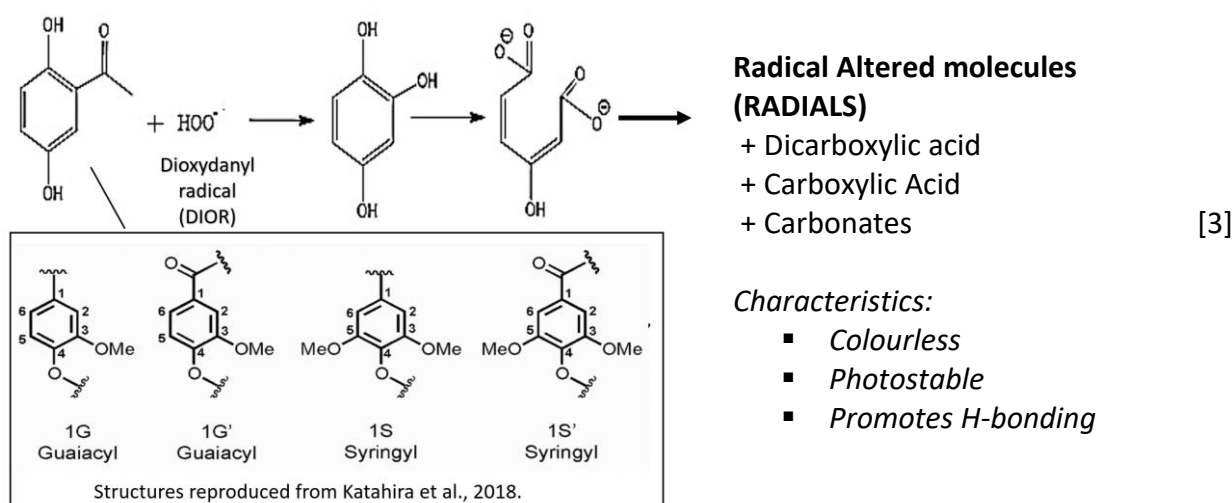


Fig. 7. Lignin monomeric units associated to RADIALS formation in reaction [3].

The possibility of being masked by the reported nano-silicates [15] at 1010 cm^{-1} is noteworthy given the huge nature of the corresponding band reported by Dormaskolla and team [27]. With the possibility of the fragments leaching into the spent liquor (reaction 2), Korntner-and-Rosenau's deliberation of the 2,5-dihydroxyacetophenone unveiled the scantiness of the component [9,10] even in fibrous mass in focus. However, correlating this with the electron microscopic analysis of the TRX-cells shed light on the possibility of zooming into the undelaminated, compact S2 layers of the microfibre, thus the inaccessibility of 2,5-dihydroxylacetophenone.

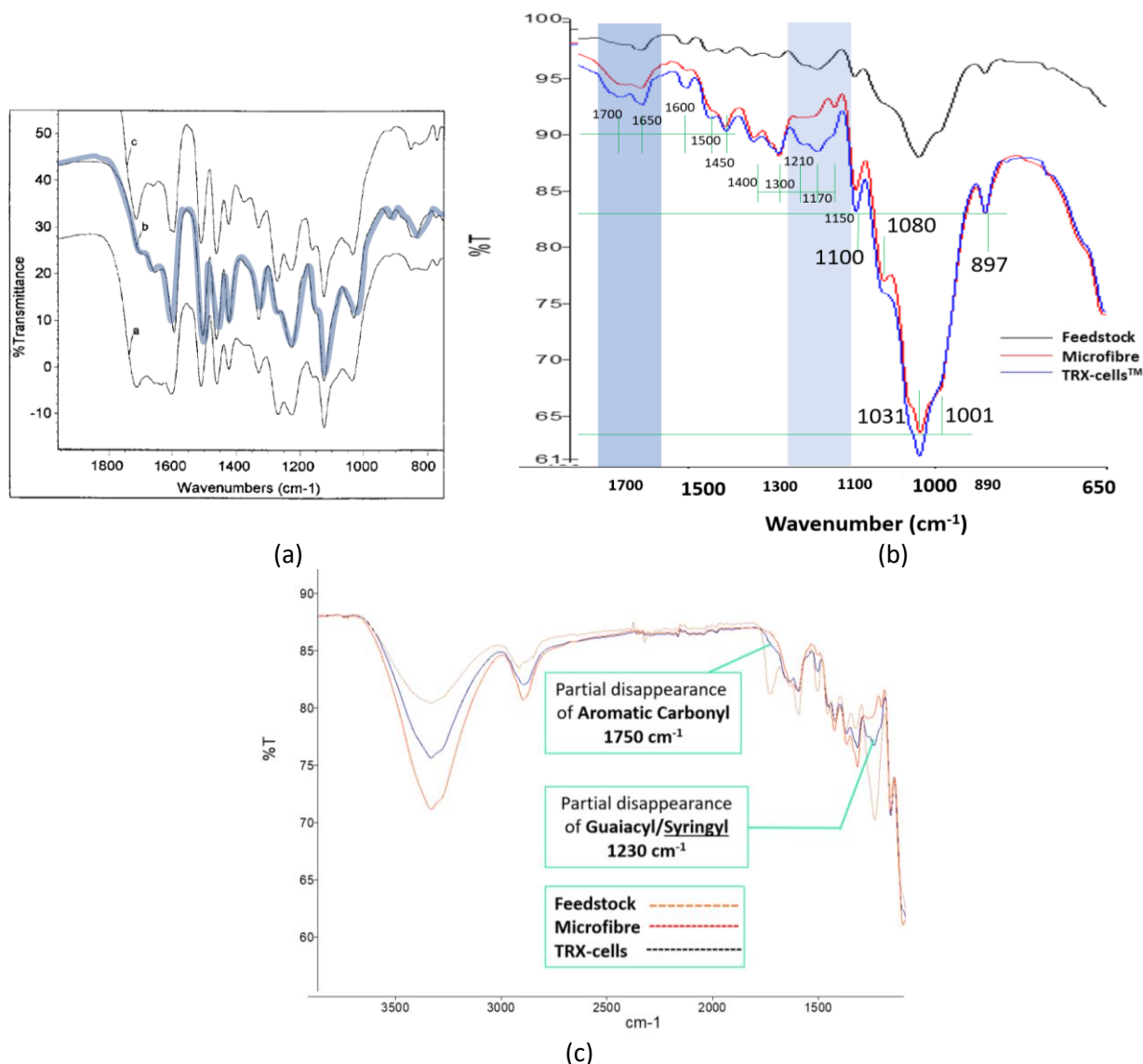


Fig. 8. FTIR bands between $1800\text{-}800\text{ cm}^{-1}$ for bands associated with (a) the lignin moiety reported by Sun *et al.*, [29], (b) DIOR residues associated with S2 multiple cell wall peeling and (c) evidence of de-aromatization and guaiacyl reduction associated with reaction 3

3.3.2 Replication

FTIR analysis of a replicate (Figure 8c) provides a slight difference insight. The disappearance of the troughs at 1750 cm^{-1} implies de-aromatization of the EFB lignin fragment while the intensity reduction of the band at 1230 cm^{-1} relative to the pattern exhibited by EFB (feedstock) is clear evidence for guaiacyl reduction.

The absence of the band corresponding to the carbonyl groups (Figure 8b) also shed light on the lignin fragment leaching from EFB, giving rise to a pH 5 spent liquor.

Analysis of the transmission band in the area reveals the influential C-O associated with syringyl and guaiacyl unit characteristics of [29]. The ultra-trace nano-bio silicate as detectable in TEM elemental analysis [15] is expected to contribute somewhat to the trough at 893 cm^{-1} , resulting in an intensity of no less than that of the β -fibre. Exposure of the nano minerals occurred because of compositional redistribution spawning from extensive PFI milling of EFB microfibre (m-fibre).

FTIR bands at 1400 cm^{-1} and 1450 cm^{-1} are characteristics of aromatic skeletal vibration corresponding to the benzyl ring, suggesting the scanty reactions involving cleavage of the aromatic ring and predominance of polyphenolics as described by Sun and co-researchers (1998) [31], pertinent to the recalcitrant S2 region that could not be penetrated by dioxydanyl radicals. Signals corresponding to the collapsed S1 layers that made the predominant mass of the TRX-cells showed evidence of de-aromatisation (1750 cm^{-1}) and guaiacyl disappearance at 1010 cm^{-1} comparison to confirming that the huge band at 1000 cm^{-1} is of feedstock origin

The huge band in 1000 cm^{-1} to 1150 cm^{-1} region reflects the C-O accumulative contribution from cellulose and silicates [25-27] in RADIALS in the m-fibre. Extensive refining of the fibrous mass via PFI milling exposed the functional group significantly, enhancing the signal depicted on the TRX-cell® mass.

The effects of compositional redistribution (arising from extensive milling) on the crystallinity of the samples in focus were also captured. FTIR analysis for crystallinity using the alkyl C-H relative to the dominating effects of O-H signals at the 1300 cm^{-1} region (Method 1) compares well with the crystallinity results determined by other methods. Comparing Method 1 to Method 2 which contrasted the aromatic C-H vs C-O reveals variability in crystallinity, which is expected of the heterogenous sample containing both cellulose and RADIALS. Table 3 presents the derived crystallinity values.

Selection of band sensitive to the amorphous and crystalline content [41] via Method 1 (Table 3) shows a high correlation of results with the crystallinity determined via the gold standard crystallographic method, X-ray Diffraction Spectroscopy [42] discussed elsewhere. Method 2 yields equivalent crystallinity values of microfibre and TRX, suggesting also a 43% crystallinity improvement following DIOR modification of biomass. The findings suggest an improved degree of structural order, regularity [43] and periodic arrangements of atoms [44] plausibly created by RADIALS and exposure of the well-ordered polymers upon refining. The increase in crystallinity was also attributable to the liberation of the less recalcitrant amorphous fines [45] as earlier reported.

Table 3
 Crystallinity Values by Crystallography and Comparative Absorbance Values

Calculation	Percentage Crystallinity Index (%)			Technique
	Microfibre	TRX	EFB	
Height ratio ($I_{1002} - I_{AM}$) / (I_{1002}) x100	70	62	38	XRD
Absorbance Ratio 1 ($[A_{2900}/A_{1372}] \times 100$)	90	63	41	FTIR
Absorbance Ratio 2 ($[A_{1420}/A_{893}] \times 100$)	61	43	43	FTIR

Table 3 presents the various options for arriving at crystallinity values with the technique of comparing the FTIR-active bonds at 2900 cm^{-1} to 1372 cm^{-1} showing the too-good-to-be-true set of values followed by the baseline corrected XRD peak height technique described by Park *et al.* [31].

Although still in the unexpectedly high crystallinity region, the CI value for EFB lies close to those normally reported for EFB [22, 23, 46].

The crystallinity ratio is potentially the marker for de-aromatisation, which may not necessarily imply crystallinity at all due to the unique properties of the DIOR-treated biomass. Relative to other biomass, the DIOR-engendered crystallinity is only 4% lower than spruce dissolving pulp reported by Ciolacu *et al.*, (2011) [20] by peak area exhibits on diffractogram. The proximation implies the suitability of the dioxydanyl-radical reaction system for amassing nano-scale functional cells from EFB.

3.4 Learning Miles at A Glimpse

The exemplified discussion on FTIR analysis is a way of actualising authentic learning involving higher-order thinking skills, problem-solving, and contextual learning achieved by breaking the circuit to verbatim copying [47, 48]. Performing analysis in authentic ways help students acquire authentic learning experience that bridges the gap to Science, Technology, Engineering and Mathematics (STEM) literacy [49] much in demand at present. The oftentimes forgotten element of STEM experiments subtly reminded in the discussion was 'replication'. By attempting more trials (or statistically, increasing 'n'), there was a higher probability for FTIR to capture the differing strata of TRX-cells. While the thick lamina of the S2 cell wall showed no sign of reaction 3 occurring, a few other spectra had captured evidence for de-aromatisation and guaiacyl reduction, plausibly exhibited by the less compact S1 layer that was soft enough for dioxydanyl radicals to penetrate. Uncovering such a correlation with theory is an important STEM motivating milestone achieved with the right footing from the beginning: analysis by the thinking journey. STRAP and the various "Delineation" stages advance the thinking activity gradually (Figure 4). The aim is to break the high-order thinking tasks into manageable energy packets to prevent duplicating ("faking") discussion and jumping to a conclusion. "Fake it till you make it" as a known way of disguising cognitive dissonance [50] is strictly prohibited in scientific tasks to avoid paralysis in the learning process.

4. Conclusions

The guideline serves as a general step to FTIR output interpretation, emphasising the initiation point (STRAP) to eliminate demotivation from handling complex spectra and the "delineation" activities to avoid excessive assumptions. Explaining the IR-active signals requires sound fundamental knowledge of the underlying reactions. The outcome enhances understanding of the complex system in focus and points to other creative use of spectroscopic signals. Comparative interpretation of FTIR spectra with the first "STraP" activities followed by finding reasons are cognitive triggers to drive further learning and avoid duplicating interpretation from the literature. The suggested STraP bridges the initiation stage to the comprehensive spectral interpretation considering all IR-active elements. Depending on the desired nature of the sample, the shown crystallinity determination using the influential crystallinity bands revealed a similar relative trend despite the varying crystallinity values that also occur within XRD - the techniques designed for crystallographic analysis. The findings alert the need to report value range rather than a single figure. At the current stage, the analytical concept requires a broad spectrum of knowledge on a similar system or background study. Once established, FTIR would potentially offer economic and rapid detection of structural changes potentially maximised as an analytical and diagnostic protocol in routine analysis.

Acknowledgement

The research on TRX-cells® is funded by The Ministry of Higher Education (MOHE) of Malaysia through Fundamental Research Grant Scheme FRGS/1/2019/STG07/USM/02/8, supporting the United Nations' Sustainable Development Goal 12, Responsible Production and Consumption.

References

- [1] Lewis, Paul D., Keir E. Lewis, Robin Ghosal, Sion Bayliss, Amanda J. Lloyd, John Wills, Ruth Godfrey, Philip Kloer, and Luis AJ Mur. "Evaluation of FTIR spectroscopy as a diagnostic tool for lung cancer using sputum." *BMC cancer* 10, no. 1 (2010): 1-10. <https://doi.org/10.1186/1471-2407-10-640>
- [2] Silva, Lidiane G., Ana FS Péres, Daniel LD Freitas, Camilo LM Morais, Francis L. Martin, Janaina CO Crispim, and Kassio MG Lima. "ATR-FTIR spectroscopy in blood plasma combined with multivariate analysis to detect HIV infection in pregnant women." *Scientific reports* 10, no. 1 (2020): 1-7. <https://doi.org/10.1038/s41598-020-77378-3>
- [3] Nogueira, Marcelo Saito, Anna Laura Barreto, Monique Furukawa, Emanuel Silva Rovai, Alice Bastos, Gabriella Bertoncetto, and Luis Felipe das Chagas e Silva. "FTIR spectroscopy as a point of care diagnostic tool for diabetes and periodontitis: A saliva analysis approach." *Photodiagnosis and Photodynamic Therapy* 40 (2022): 103036. <https://doi.org/10.1016/j.pdpdt.2022.103036>
- [4] Finlayson, Duncan, Christopher Rinaldi, and Matthew J. Baker. "Is infrared spectroscopy ready for the clinic?." *Analytical chemistry* 91, no. 19 (2019): 12117-12128. <https://doi.org/10.1021/acs.analchem.9b02280>
- [5] Al Mayadeen English. "Indonesia, Malaysia to defend palm oil from EU 'discriminatory' ban." *Al Mayadeen English* January 10, 2023.
- [6] Jalil, Asila. "SD Plantation responds to RSPO's directives to complete the action plan." *New Strait Times*. November 21, 2022.
- [7] Fai, Soon Zheng, and Choon Yoong Cheok. "Physical and chemical characterization of oil extracted from *Citrofortunella microcarpa*, *Hibiscus sabdariffa* and *Artocarpus heterophyllus* seeds." *Progress in Energy and Environment* 22 (2022): 1-12. <https://doi.org/10.37934/progee.22.1.112>
- [8] Mohammad, Intan Nazirah, Clarence M. Ongkudon, and Mailin Misson. "Physicochemical properties and lignin degradation of thermal-pretreated oil palm empty fruit bunch." *Energies* 13, no. 22 (2020): 5966. <https://doi.org/10.3390/en13225966>
- [9] Rosenau, Thomas, Antje Potthast, Andreas Hofinger, and Paul Kosma. "Isolation and identification of residual chromophores in cellulosic materials." In *Macromolecular Symposia*, vol. 223, no. 1, pp. 239-252. Weinheim: WILEY-VCH Verlag, 2005. <https://doi.org/10.1002/masy.200550517>
- [10] Korntner, Philipp, Takashi Hosoya, Thomas Dietz, Klaus Eibinger, Heidemarie Reiter, Martin Spitzbart, Thomas Röder et al. "Chromophores in lignin-free cellulosic materials belong to three compound classes. Chromophores in celluloses, XII." *Cellulose* 22, no. 2 (2015): 1053-1062. <https://doi.org/10.1007/s10570-015-0566-6>
- [11] Dermawan, Yunita Megasari, Arniza Ghazali, W. D. Wan Rosli, Mohd Ridzuan Hafiz Mohd Zukeri, and Nurul Hasanah Kamaluddin. "Alkaline Peroxide in Synergy with Mechanical Refining as Factor in the Development of EFB Paper Properties." In *Advanced Materials Research*, vol. 832, pp. 488-493. Trans Tech Publications Ltd, 2014. <https://doi.org/10.4028/www.scientific.net/AMR.832.488>
- [12] Ghazali, Arniza, and Marcin Zbiec. "Rich Dad and Poor Dad: Biomass Circularity Science Empathizing Rubber Smallholders." *Journal of Advanced Research in Applied Sciences and Engineering Technology* 29, no. 1 (2022): 207-222. <https://doi.org/10.37934/araset.29.1.207222>
- [13] Ibrahim, Mohd Nasir Mohd. "Vanilla from Black Liquor." *Bulletin Kimia*. 2013.
- [14] Kresnowati, M. T. A. P., D. Lestari, M. Anshori, and R. M. Jafar. "Production of carotenoids from oil palm empty fruit bunches." In *IOP Conference Series: Earth and Environmental Science*, vol. 460, no. 1, p. 012025. IOP Publishing, 2020. <https://doi.org/10.1088/1755-1315/460/1/012025>
- [15] Ghazali, Arniza, N. Azhar, S. H. A. H. R. O. M. Mahmud, M. F. A. M. Khairudin, Ishak Ahmad, Mohd Rafatullah, Muhammad Al Amin Zaini, and Y. U. S. H. A. M. D. A. N. Yusof. "Delaminated Cells for Nano-enabled Inkjet Printability." *Cellulose Chemistry and Technology* (2021). <https://doi.org/10.35812/cellulosechemtechnol.2021.55.92>
- [16] Ghazali, Arniza, Rabeta Mohd Salleh, Mohd Qasimie Ahmad, Nurhaffizah Azhar, and Muhammad Fadhurul Abd Malik. "Capturing Anthocyanin Immobilization On Rice Through The Ultra-High Resolution Electron Lenses." *Malaysian Journal of Microscopy* 17, no. 2 (2021).

- [17] Zulkifli, Mohamad Dzulhilmi, Mostafa Yusefi, and Kamyar Shameli. "Curcumin Extract Loaded with Chitosan Nanocomposite for Cancer Treatment." *Journal of Research in Nanoscience and Nanotechnology* 6, no. 1 (2022): 1-13. <https://doi.org/10.37934/jrnn.6.1.113>
- [18] Kruer-Zerhusen, Nathan, Borja Cantero-Tubilla, and David B. Wilson. "Characterization of cellulose crystallinity after enzymatic treatment using Fourier transform infrared spectroscopy (FTIR)." *Cellulose* 25, no. 1 (2018): 37-48. <https://doi.org/10.1007/S10570-017-1542-0>
- [19] Pędziwiatr, Paulina, Filip Mikołajczyk, Dawid Zawadzki, Kinga Mikołajczyk, and Agnieszka Bedka. "Decomposition of Hydrogen Peroxide – Kinetics and Review of Chosen Catalysts." *Acta Innovations* 26, (2018):45-52. <https://doi.org/10.32933/ActaInnovations.26.5>
- [20] Ciolacu, Diana, Florin Ciolacu, and Valentin I. Popa. "Amorphous cellulose—structure and characterization." *Cellulose chemistry and technology* 45, no. 1 (2011): 13.
- [21] Fengel, Dietrich, Hannes Jakob, and Claudia Strobel. "Influence of the alkali concentration on the formation of cellulose II. Study by X-ray diffraction and FTIR spectroscopy." (1995): 505-511. <https://doi.org/10.1515/hfsg.1995.49.6.505>
- [22] Fatah, Ireana Yusra A., H. P. S. Abdul Khalil, Md Sohrab Hossain, Astimar A. Aziz, Yalda Davoudpour, Rudi Dungani, and Amir Bhat. "Exploration of a chemo-mechanical technique for the isolation of nanofibrillated cellulosic fiber from oil palm empty fruit bunch as a reinforcing agent in composites materials." *Polymers* 6, no. 10 (2014): 2611-2624. <https://doi.org/10.3390/polym6102611>
- [23] Rosazley, R., M. Z. Shazana, M. A. Izzati, A. W. Fareezal, I. Rushdan, and Z. M. A. Ainun. "Characterization of nanofibrillated cellulose produced from oil palm empty fruit bunch fibers (OPEFB) using ultrasound." *Journal of Contemporary Issues and Thought* 6 (2016): 30-37.
- [24] Ferrer, Ana, Ilari Filpponen, Alejandro Rodríguez, Janne Laine, and Orlando J. Rojas. "Valorization of residual Empty Palm Fruit Bunch Fibers (EPFBF) by microfluidization: production of nanofibrillated cellulose and EPFBF nanopaper." *Bioresource technology* 125 (2012): 249-255. <https://doi.org/10.1016/j.biortech.2012.08.108>
- [25] Nandiyanto, Asep Bayu Dani, Rosi Oktiani, and Risti Ragadhita. "How to read and interpret FTIR spectroscopy of organic material." *Indonesian Journal of Science and Technology* 4, no. 1 (2019): 97-118. <https://doi.org/10.17509/ijost.v4i1.15806>
- [26] Terzioğlu, P., Sevil Yücel, and Didem Özçimen. "The utilization of wheat hull ash for the production of barium and calcium silicates." *Latin American applied research* 43, no. 4 (2013): 319-324.
- [27] Darmakkolla, Srikar Rao, Hoang Tran, Atul Gupta, and Shankar B. Rananavare. "A method to derivatize surface silanol groups to Si-alkyl groups in carbon-doped silicon oxides." *RSC advances* 6, no. 95 (2016): 93219-93230. <https://doi.org/10.1039/C6RA20355H>
- [28] Zwirchmayr, Nele S., Ute Henniges, Markus Bacher, Takashi Hosoya, Heidemarie Reiter, Martin Spitzbart, Thomas Dietz et al. "Degradation of the cellulosic key chromophores 2, 5-and 2, 6-dihydroxyacetophenone by hydrogen peroxide under alkaline conditions. Chromophores in cellulose, XVII." *Cellulose* 25, no. 7 (2018): 3815-3826. <https://doi.org/10.1007/s10570-018-1817-0>
- [29] Sun, R. C., J. M. Fang, and J. Tomkinson. "Fractional isolation and structural characterization of lignins from oil palm trunk and empty fruit bunch fibers." *Journal of wood chemistry and technology* 19, no. 4 (1999): 335-356. <https://doi.org/10.1080/02773819909349616>
- [30] Katahira, Rui, Thomas J. Elder, and Gregg T. Beckham. "A brief introduction to lignin structure." (2018): 1-20. <https://doi.org/10.1039/9781788010351-00001>
- [31] Sun, Yan-Ping, Kien Loi Nguyen, and Adrian FA Wallis. "Ring-opened products from reaction of lignin model compounds with UV-assisted peroxide." (1998): 61-66. <https://doi.org/10.1515/hfsg.1998.52.1.61>
- [32] Thulluri, Chiranjeevi, Ravi Balasubramaniam, and Harshad Ravindra Velankar. "Generation of highly amenable cellulose-I β via selective delignification of rice straw using a reusable cyclic ether-assisted deep eutectic solvent system." *Scientific reports* 11, no. 1 (2021): 1-14. <https://doi.org/10.1038/s41598-020-80719-x>
- [33] Park, Sunkyu, John O. Baker, Michael E. Himmel, Philip A. Parilla, and David K. Johnson. "Cellulose crystallinity index: measurement techniques and their impact on interpreting cellulase performance." *Biotechnology for biofuels* 3, no. 1 (2010): 1-10. <https://doi.org/10.1186/1754-6834-3-10>
- [34] Fryhle, Craig B., and Scott A. Snyder. *Organic chemistry*. John Wiley & Sons, 2022.
- [35] TAPPI, (Technical Association for Pulp and Paper Industry) (1997) TAPPI Standard Methods. 1997, USA.
- [36] Sun, RunCang, Jeremy Tomkinson, and James Bolton. "Effects of precipitation pH on the physico-chemical properties of the lignins isolated from the black liquor of oil palm empty fruit bunch fibre pulping." *Polymer degradation and stability* 63, no. 2 (1999): 195-200. [https://doi.org/10.1016/S0141-3910\(98\)00091-3](https://doi.org/10.1016/S0141-3910(98)00091-3)
- [37] Ghazali, Arniza, W. D. Wanrosli, and Kwei-Nam Law. "Alkaline Peroxide Mechanical Pulping (APMP) of Oil Palm Lignocellulose: Part 2-Empty Fruit Bunch (EFB) Responses to Pretreatments." *Appita: Technology, Innovation, Manufacturing, Environment* 59, no. 1 (2006): 65-70.

- [38] Khairil, Mohd Azli Mat Lazin, Arniza Ghazali, and Wan Rosli Wan Daud "Effects of alkaline peroxide percentages on the handsheets made from the alkaline peroxide pulp of EFB." *JIRCAS Working Report*, 73 (2012):166-171. Publisher: Japan International Research Center for Agricultural Sciences.
- [39] Ghazali, Arniza, Mohd Ridzuan Hafiz Mohd Zukeri, W. D. Wan Rosli, Baharin Azahari, Rushdan Ibrahim, Issam Ahmed Mohamed, Tanweer Ahmad, and Ziya Ahmad Khan. "Augmentation of EFB fiber web by nano-scale fibrous elements." In *Advanced Materials Research*, vol. 832, pp. 494-499. Trans Tech Publications Ltd, 2014. <https://doi.org/10.4028/www.scientific.net/AMR.832.494>
- [40] Hinterstoisser, Barbara, and Lennart Salmén. "Application of dynamic 2D FTIR to cellulose." *Vibrational Spectroscopy* 22, no. 1-2 (2000): 111-118. [https://doi.org/10.1016/S0924-2031\(99\)00063-6](https://doi.org/10.1016/S0924-2031(99)00063-6)
- [41] Partini, Maria, and Roberto Pantani. "Determination of crystallinity of an aliphatic polyester by FTIR spectroscopy." *Polymer Bulletin* 59, no. 3 (2007): 403-412. <https://doi.org/10.1007/s00289-007-0782-9>
- [42] Querido, William, Ramyasri Ailavajhala, Mugdha Padalkar, and Nancy Pleshko. "Validated approaches for quantification of bone mineral crystallinity using transmission Fourier transform infrared (FT-IR), attenuated total reflection (ATR) FT-IR, and Raman spectroscopy." *Applied spectroscopy* 72, no. 11 (2018): 1581-1593. <https://doi.org/10.1177/0003702818789165>
- [43] Shrivastava, Anshuman. *Introduction to plastics engineering*. William Andrew, 2018. <https://doi.org/10.1016/B978-0-323-39500-7.00001-0>
- [44] Abhilash, Venkateshaiah, Nutenki Rajender, and Kattimuttathu Suresh. "X-ray diffraction spectroscopy of polymer nanocomposites." In *Spectroscopy of Polymer Nanocomposites*, pp. 410-451. William Andrew Publishing, 2016. <https://doi.org/10.1016/B978-0-323-40183-8.00014-8>
- [45] Kamaludin, Nurul H., Arniza Ghazali, and Wan Daud Wanrosli. "Potential of fines as reinforcing fibres in alkaline peroxide pulp of oil palm empty fruit bunch." *BioResources* 7, no. 3 (2012): 3425-3438.
- [46] Padzil, Farah Nadia Mohammad, Seng Hua Lee, Zuriyati Mohamed Asa'ari Ainun, Ching Hao Lee, and Luqman Chuah Abdullah. "Potential of oil palm empty fruit bunch resources in nanocellulose hydrogel production for versatile applications: A review." *Materials* 13, no. 5 (2020): 1245. <https://doi.org/10.3390/ma13051245>
- [47] Ibegbulam, Ijeoma J., and Jacintha U. Eze. "Knowledge, perception and attitude of Nigerian students to plagiarism: A case study." *IFLA journal* 41, no. 2 (2015): 120-128. <https://doi.org/10.1177/0340035215580278>
- [48] Ghazali, Arniza, and Azniwati Abdul Aziz. "Resetting Integrity Through Communication on Plagiarism: University Classrooms Weaving Values into the Social Fabric." *International Journal of Learning, Teaching and Educational Research* 20, no. 12 (2021). <https://doi.org/10.26803/ijlter.20.12.13>
- [49] Foj, Liew Yon, and Teoh Hong Kean. "STEM education in Malaysia: An organisational development approach?." *International Journal of Advanced Research in Future Ready Learning and Education* 29, no. 1 (2022): 1-19.
- [50] Pressable. "Fake It Till You Make It: Is It Really Good Advice?" *Science of People*.